ELSEVIER

Biochimica et Biophysica Acta 1543 (2000) 253–274

BIOCHIMICA ET BIOPHYSICA ACTA
BBA

www.elsevier.com/locate/bba

Review

Protein engineering of bacterial α-amylases

Jens Erik Nielsen [a], Torben V. Borchert [b,*]

[a] *EMBL, Meyerhofstrasse 1, 69117 Heidelberg, Germany*
[b] *Enzyme Design, Novozymes A/S, Novo Alle, 2880 Bagsværd, Denmark*

Received 9 February 2000; received in revised form 21 September 2000; accepted 28 September 2000

Abstract

α-Amylases constitute a very diverse family of glycosyl hydrolases that cleave α1→4 linkages in amylose and related polymers. Recent structural and mutagenic studies of archeael, mammalian and bacterial α-amylases have resulted in a wealth of information on the catalytic mechanism and on the structural features of this enzyme class. Because of their high thermo-stability, the *Bacillus* α-amylases have found widespread use in industrial processes, and much attention has been devoted to optimising these enzymes for the very harsh conditions encountered there. Stability has been a major area of focus in this respect, and several remarkably stable bacterial α-amylases have been produced by bioengineering techniques. Protein engineering studies of pH-activity profiles and of substrate specificities have also been initiated, although without much success. In the coming years it is likely, however, that the focus of α-amylase engineering will shift from engineering stability to these new areas.

Keywords: Protein engineering; α-Amylase; Thermostability; Stability engineering; pH activity profile

1. Introduction

The glycolytic pathway and the citric acid cycle stand as paradigms for energy producing pathways in cells. These pathways show a great deal of variability between organisms, but many of the core enzymes of both glycolysis and the citric acid cycle seem to be conserved in the vast majority of organisms whose genomes have been sequenced [1,2]. Glycolysis is responsible for the breakdown of sugars, in particular glucose, and the conservation of this pathway thus suggests that glucose is a major source of energy for many organisms. Glucose is found in nature in large quantities, primarily in a polymeric state as cellulose (β1→4 linked) and as starch and glycogen (both α1→4 linked). Cellulose and starch are produced predominantly in higher plants, and glycogen is the main sugar storage polymer in animals [3]. Enormous amounts of glucose are therefore available to organisms that can hydrolyse glucose polymers efficiently. This has, of course, not been overlooked by evolution, and the multitude and diversity found among glucose-polymer hydrolysing enzymes [4] show the significance that glucose polymers have for life.

Abbreviations: AHA, *Alteromona haloplanctis* α-amylase; CGTase, cyclodextrin glycosyl transferase; PPA, pig pancreatic α-amylase; BAA, *Bacillus amyloliquefaciens* α-amylase; BLA, *Bacillus licheniformis* α-amylase; BstA, *Bacillus stearothermophilus* α-amylase

* Corresponding author. Fax: +45-4498-0246;
E-mail: tvb@novozymes.com

0167-4838/00/$ – see front matter
PII: S0167-4838(00)00240-5

Humans do not produce enzymes that can hydrolyse glucose β1→4 linkages, and consequently trees and other predominantly cellulose-containing plants are not part of the standard human diet. Plants that contain starch such as rice and potatoes are, on the other hand, digested very well by humans, which is due to the presence of starch-hydrolysing enzymes in both saliva and the gastrointestinal tract [5,6].

Of the starch-hydrolysing enzymes, the α-amylases (EC 3.2.1.1) are of special importance as they are responsible for the solubilisation of starch. Starch consists of two glucose polymers: amylose, which is exclusively α1→4 linked, and amylopectin which, in addition to the α1→4 linkages found in amylose, also contains many α1→6 branch points [3,7]. The α-amylases catalyse the hydrolysis of internal α1→4 glycosidic linkages and are thus ideally suited to cutting a starch polymer into smaller fragments. They are found in both eubacteria and eukaryota and have a large number of different substrate specificities as well as a huge variation in both temperature and pH optima [3]. The bacterial and fungal α-amylases, and especially the enzymes from the *Bacillus* species, have found widespread use in industrial processes because of their high thermo-stability, but the efficient expression systems [8] have also made them attractive for such purposes.

The bacterial α-amylases are evolutionarily quite distant from the eukaryotic enzymes, with the sequence identity to pig pancreatic α-amylase (PPA) being in the range of 15–20% for most enzymes. An exception to this is the *Alteromonas haloplanctis* α-amylase (AHA), which has around 50% sequence identity to PPA [9]. Most *Streptomyces* enzymes also have sequence identities to PPA in the range of 40–50% (data not shown). Among the α-amylases, the bacterial enzymes are the most diverse as far as physio-chemical properties are concerned. The most notable are the temperature-activity optima that range from approximately 25°C [10] (AHA) to around 90°C [11] (*Bacillus licheniformis* α-amylase [BLA]). The bacterial α-amylases display activity from pH 1.0 (*Bacillus sp*. [12]) to approximately pH 11.5 (*Bacillus* No. A-40-2 α-amylase [13]), and the substrate specificity varies both in the preference for chain length and in the ability to cleave close to the α1→6 branch points in amylopectin and other branched glucose polymers [3,7,14,15].

2. Industrial uses

Starch-hydrolysing enzymes and α-amylases in particular are used in a number of industrial processes [7]. α-Amylases are, for example, used for starch hydrolysis in the starch liquefaction process that converts starch into fructose and glucose syrups. They are also used as a partial replacement for the expensive malt in the brewing industry, to improve flour in the baking industry, and to produce modified starches for the paper industry. In addition to this, they are used to remove starch in the manufacture of textiles (desizing) and as additives to detergents for both washing machines and automated dish-washers. Each of these processes take place under physical and chemical conditions that are quite diverse. Two examples of the harsh conditions encountered by α-amylases in industrial applications will be described in more detail below.

2.1. Detergents

As low and medium-temperature laundering becomes more common, the removal of stains that contain starch from clothes and porcelain has become increasingly problematic for the consumer, as the solubility of starch is highly dependent on temperature. This has resulted in the increased use of α-amylases in detergents. The use of α-amylases in detergents is problematic as detergents make rather severe demands on the enzymes added with respect to stability and activity. For example the pH is often very alkaline (it can be as high as 10.5) and the washing environment can be very oxidising. Furthermore, the enzymes have to withstand the surfactants, metal ion chelating agents and proteases that are often also added to the detergent.

2.2. Starch liquefaction

α-Amylases are also used in the starch liquefaction process, which serves as an example of a quite different set of application conditions. The conversion of starch into maltodextrins is the first step in this process that converts, e.g., corn starch to a fructose/glucose syrup. The rapid liquefaction of the starch that takes place simultaneously with steam injection is absolutely necessary for reducing the viscosity of

the 40% starch slurry. The process is currently carried out at approximately pH 6, but it is desirable to lower the pH value even further in order to limit the formation of by-products.

Formerly only a few α-amylases were commercially available for meeting the very diverse application conditions illustrated by the two examples above. A single α-amylase will obviously not be able to meet the particular demands of every industrial process, and the optimisation of α-amylases for each individual application by means of bioengineering techniques is therefore desirable. Optimising an α-amylase for a single application is often time-consuming and problematic, and many industrial processes are thus still carried out with 'unoptimised' enzymes. Significant progress has, however, been made in the optimisation of α-amylases for the use in the starch liquefaction process and detergent powders, especially in terms of thermo-stability.

3. Classification of enzymes displaying α-amylase activity

The Enzyme Commission (EC) classification of enzymes is based on naming the reaction catalysed. Each reaction is consequently assigned an EC number that uniquely identifies the reaction. For the α-amylases this number is 3.2.1.1 and the reaction is described as the 'endohydrolysis of 1,4-α-glucosidic linkages in oligosaccharides and polysaccharides'.

Enzymes that catalyse very similar reactions are assigned different EC numbers. The cyclodextrin glucanotransferases (CGTases), for example, have a their own EC number (2.4.1.19), although they are structurally and enzymatically very similar to the α-amylases [16,17]. α-glucosidases (3.2.1.20), maltogenic α-amylases (glucan 1,4-α-maltohydrolases EC 3.2.1.133) and maltotetraose-forming amylases (glucan 1,4-α-maltotetrahydrolase EC 3.2.1.60), which all have structures and enzymatic properties that are very similar to the α-amylases, are likewise not classified with the α-amylases because they are exo-enzymes.

Even though the EC system is very useful for classification purposes, it often makes sense to include enzymes from several EC classes when studying a particular enzyme class. This is especially true of the starch-hydrolysing enzymes, as the boundaries between the different substrate/product specificities for these enzymes are hard to define. Thus, CGTases hydrolyse part of their substrates, making them act exactly like α-amylases [17], while some α-amylases display possessiveness or multiple attack behaviour [18], which makes them act as maltogenic α-amylases or as maltotetraose-forming amylases.

When trying to understand α-amylases, not only the data on α-amylases in the rather strict EC definition should be included. All available information should be used as long as the enzymes in question display similar enzymatic and structural characteristics with regard to the property that is of interest.

This was realised quite early on by Henrissat [19], who initiated the construction of the Carbohydrate Active Enzymes (CAZy) database [4]. This database holds information on the classification of glycosyl hydrolases according to their sequence. Enzymes with α-amylase activity are found in two structurally different glycosyl hydrolase families in this database, namely families 13 and 57.

Family 13 contains 514 sequences and 19 different enzyme activities. Among these are the CGTases, the

Table 1
List of bacterial α-amylase X-ray structures

PDB identifier	Molecule	Source	Resolution	Ligand	Remarks
1AQM	α-Amylase	*Alteromonas haloplanctis*	1.85	Ca^{2+}, Cl^- Tris	
1AQH	α-Amylase	*Alteromonas haloplanctis*	2.00	Ca^{2+}, Cl^-	
1BPL	α-Amylase	*Bacillus licheniformis*	2.20		Calcium depleted
1VJS	α-Amylase	*Bacillus licheniformis*	1.70		Calcium depleted
1BLI	α-Amylase	*Bacillus licheniformis*	1.90	3 Ca^{2+} 1 Na^+	Mutations: N190F, Q264S, N265Y
1BAG	α-Amylase	*Bacillus subtilis*	2.50	3 Ca^{2+} DP5	Mutation: E208Q

DP5, Maltopentaose.

Fig. 1. The domain organisation of the α-amylases and related enzymes. Domain A is shown in green, domain B is shown in magenta and domain C is shown in cyan. Calcium ions and sodium ions are shown as red spheres and orange spheres respectively. (A) *Bacillus licheniformis* α-amylase (PDB code 1BLI). The active site residues Asp231, Glu261 and Asp328 are shown in red. The loop connecting β7 to α7 is shown in yellow. (B) *Bacillus subtilis* α-amylase (PDB code 1BAG) with maltopentaose (yellow) bound in the active site. (C) *Alteromona haloplanctis* α-amylase (PDB code 1AQH). The four disulphide bridges and the chloride ion in the active site are shown in yellow. (D) maltotetraose-forming α-amylase from *Pseudomonas stutzeri* (PDB code 1JDC with maltotetraose in the active site. (E) Cyclodextrin glycosyl transferase from *Bacillus circulans* (PDB code 1CXE) with maltotriose in the active site. Domains D and E are shown in white and yellow, respectively. The figures were prepared with the Molscript [89] and Raster3D [90] programs.

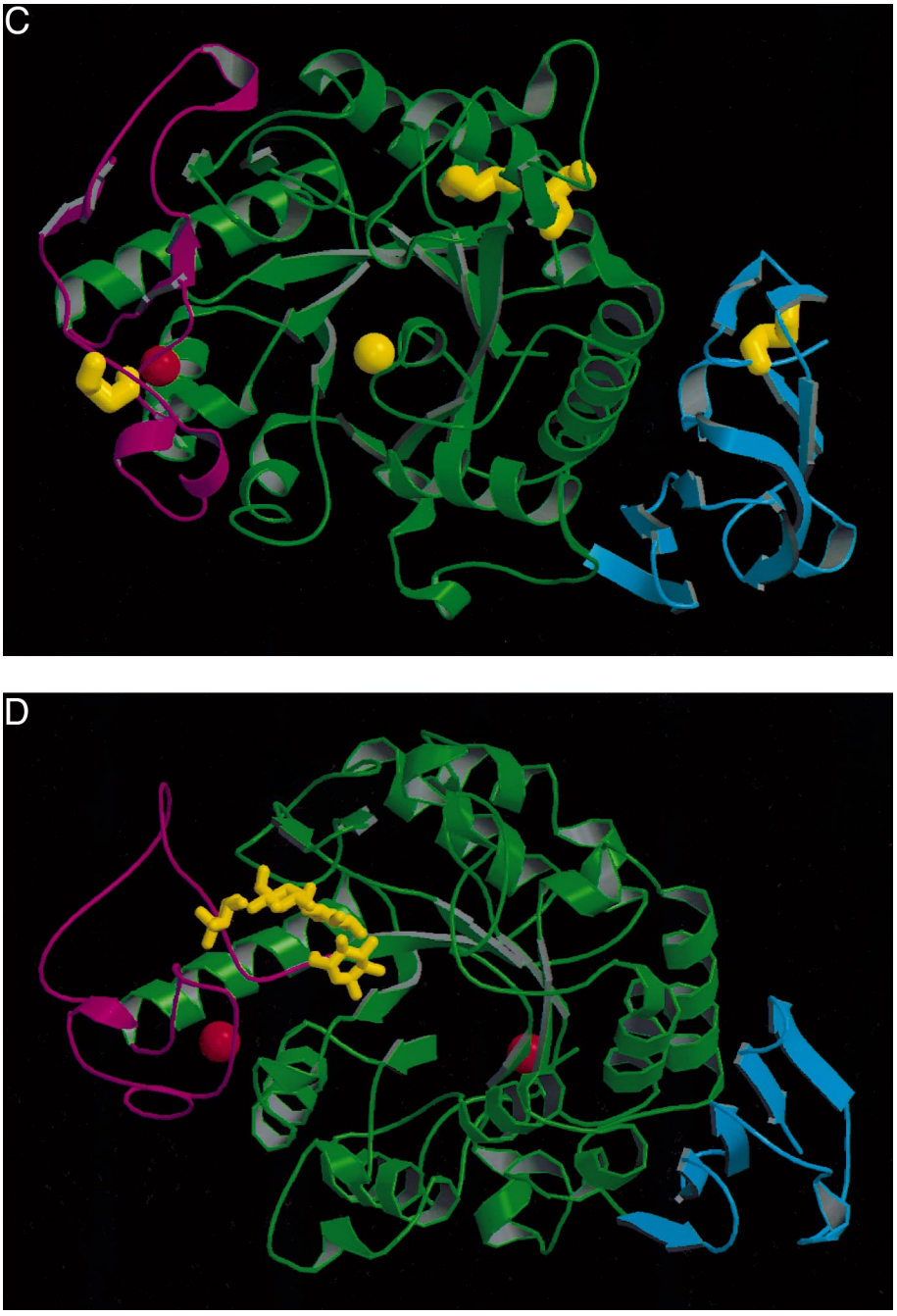

Fig. 1 (*continued*).

α-glucosidases and the maltotetraose-forming amylases. Presently, 73 X-ray structures are available for this family, making it the most studied enzyme family in the CAZy database (see Table 1 for a list of bacterial α-amylase X-ray structures).

Family 57, on the other hand, comprises only 13 sequences and only two different enzyme activities, namely the α-amylase activity (EC 3.2.1.1) and the 4-α-glucanotransferase activity (EC 2.4.1.-). No X-ray structures are available for any of the enzymes in this family, and it is generally less well characterised than family 13.

The α-amylases belonging to family 57 are likely to have completely different structural and enzymatic

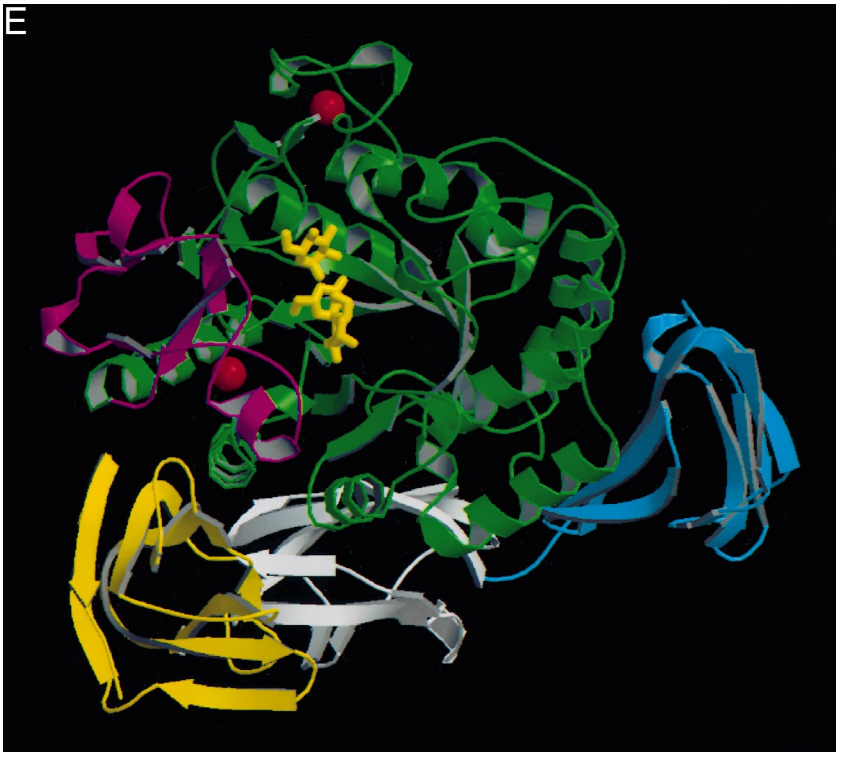

Fig. 1 (*continued*).

features than the enzymes in family 13. We therefore consider these enzymes to be outside the scope of this review.

4. Structure

X-ray studies of mammalian and bacterial α-amylases (see Table 1) have shown that all α-amylases consist of three domains, called A, B and C (Fig. 1). A central $(\alpha/\beta)_8$ TIM-barrel (domain A) forms the core of the molecule and contains the three active site residues Asp231, Glu261 and Asp328 (*Bacillus licheniformis* α-amylase [BLA] numbering). Domains B and C are located roughly at opposite sides of this TIM-barrel. Domain B is formed by a protrusion between the third strand and the third helix of the TIM-barrel. Domain B has a rather irregular β-rich structure, and varies substantially in size and structure among the α-amylases [20]. Domain B forms a large part of the substrate binding cleft and is presumed to be important for the substrate specificity differences observed between α-amylases [21]. Domain C constitutes the C-terminal part of the sequence and is a β-sandwich domain containing a Greek key motif. Mammalian α-amylases contain several disulphide bridges, but the bacterial enzymes are generally devoid of these. The AHA, however, contains four disulphide bridges, thereby also resembling the mammalian enzymes in this respect [9].

4.1. Calcium and sodium ions

All known α-amylases contain a conserved calcium ion, which is located at the interface between domains A and B [22–24] and which is known to be essential for having a stable, active enzyme [25]. The calcium ion is bound very tightly as is shown by the dissociation constants for PPA and AHA, which have been measured to 44 nM [26] and 0.0050 nM [27] respectively. It has been suggested that the role of the conserved calcium ion is mainly structural [24,28,29] since it is too far away from the active site to participate directly in catalysis.

One or more additional calcium ions have been found in several structures [22,24,30], and a particularly interesting case is the linear Ca–Na–Ca arrangement found in BLA [24,31]. X-ray structures are

available for both the calcium-depleted wild type and for a threefold mutant of this enzyme [23,24]. This has allowed Machius et al. [24] to propose a disorder → order transition that should supposedly occur when Ca^{2+} is bound to the calcium-depleted form of the enzyme [23]. It is unknown, however, whether the calcium-depleted α-amylase can be reactivated by the addition of calcium, thus making the disorder → order transition theory hypothetical.

4.2. Chloride ions

Several α-amylases contain a chloride ion in the active site, which has been shown to enhance the catalytic efficiency of the enzyme, presumably by elevating the pK_a of the hydrogen-donating residue in the active site (see below; [27,32]). Chloride ions have been found mainly in mammalian α-amylases [5,6,28], although a chloride ion has also been reported in a psychrophilic α-amylase (AHA) from the *Alteromonas haloplanctis* bacterium [9]. It has been observed that the affinity for the conserved calcium ion increases dramatically upon chloride binding [27], and it is therefore conceivable that chloride ion binding also induces conformational changes around the active site.

A puzzling feature of chloride containing α-amylases is a serine protease-like Glu–His–Ser triad in the interface between domains A and C. Aghajari et al. [9] propose that this triad is capable of performing an autoproteolytic cleavage. The experimental evidence for an autoproteolytic event is mostly indirect [9], and the hypothesis thus still awaits experimental confirmation.

4.3. The active site cleft

The active site cleft is located in the interface between domain A and domain B, and is found at the C-terminal end of the β-strands in the TIM barrel. X-ray structures of α-amylases complexed with the inhibitory pseudo tetra-saccharide acarbose has shown that the substrate binding cleft can accommodate from four to ten glucose units (depending on species). Each glucose unit is bound by certain of the amino acid residues said to constitute the binding subsite for that glucose unit. Subsite nomenclature has been defined by Davies et al. [33], i.e., subsites are numbered according to the location of the scissile bond, with negative subsite numbers on the non-reducing side of the scissile bond (see Fig. 2).

In the α-amylases there are two or three subsites present on the reducing end of the scissile bond (subsites +1, +2 and +3), whereas the number of subsites on the non-reducing side of scissile bond varies between two and seven [21,31].

The X-ray structures of α-amylases in complex with acarbose show the acarbose occupying subsites −1 to +4. Density for one or more sugar units in addition to the density for the four sugar units from acarbose are, however, often seen in these X-ray structures [34,35]. Until recently it was unclear whether the electron density originated from a longer sugar molecule resulting from a transglycosylation event or from acarbose units positioned differently in the individual protein molecules. A study on a chimaeric *Bacillus* α-amylase (BA2) has settled this issue [31], concluding that the extra density does indeed originate from a transglycosylation event that produces longer chained sugar molecules. In the BA2 structure a deca-saccharide molecule is found in the active site cleft spanning subsites −7 to +3. It is interesting to note that in an active site mutant of BA2 [31], a native, highly disordered acarbose moiety was found that spanned subsites −7 to −4. This result suggests that the catalytic activity of the α-amylases is necessary in order to convert acarbose into a more potent longer-chained inhibitor.

Attempts have been made to change the substrate and product specificity of bacterial α-amylases, most notably by Vihinen et al. [36], who achieved a significant alteration of the end product composition for *Bacillus stearothermophilus* α-amylase by protein engineering techniques. Other studies on the substrate/product specificity of bacterial α-amylases include those by Takase [37], Dua and Kochhar [38] and Suganuma et al. [39]. The substrate specificity

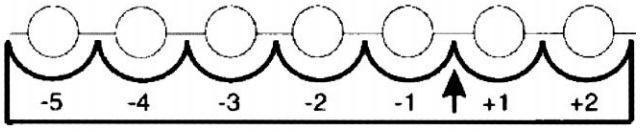

Fig. 2. Active site cleft subsite nomenclature for glycosyl hydrolases as defined by Davies et al. [33]. The non-reducing end of the sugar is to the left. The arrow indicates the scissile bond.

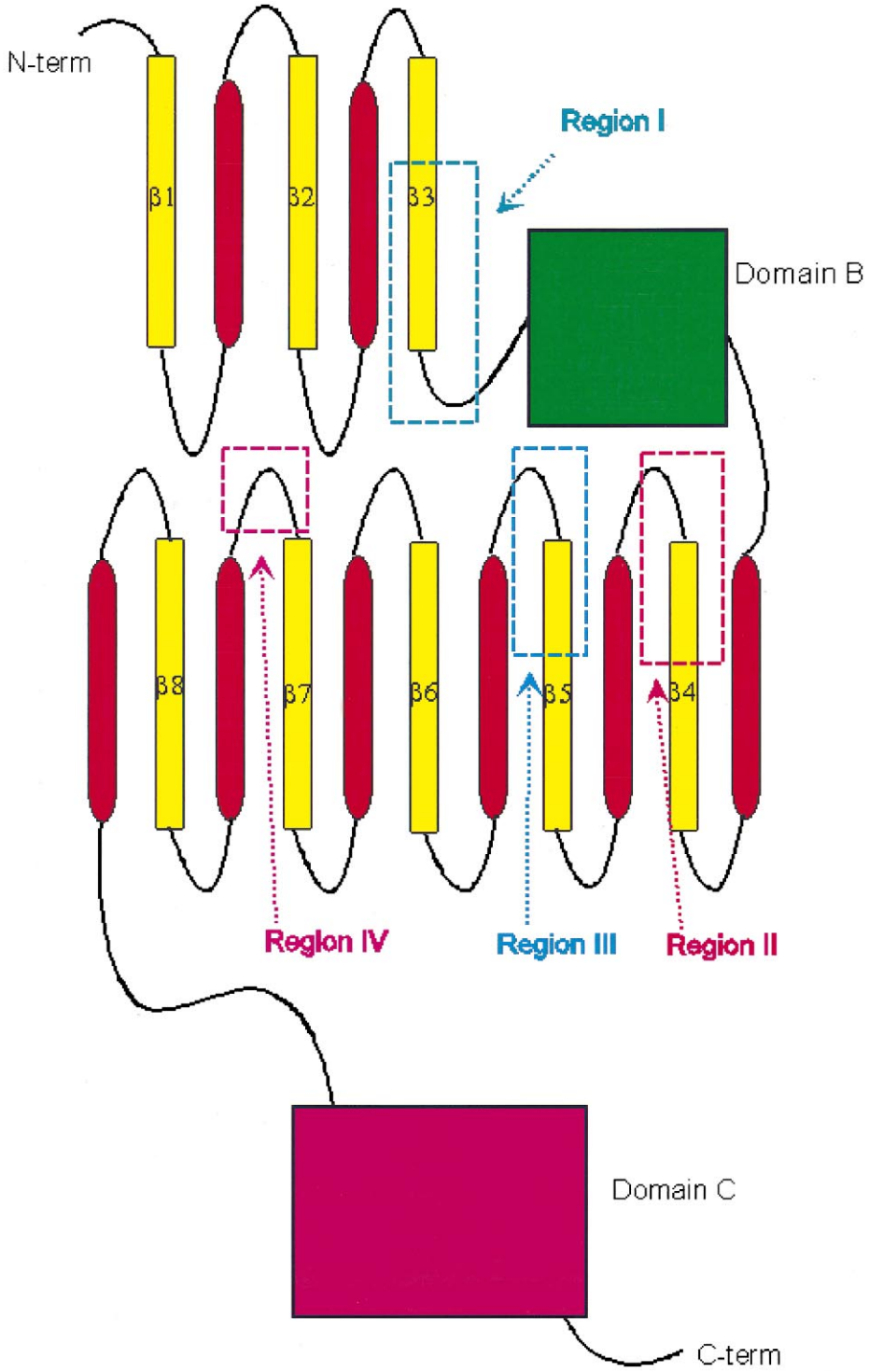

Fig. 3. Topology diagram of α-amylases. The positions of the four conserved sequence patterns (Fig. 4) are indicated with dashed boxes.

studies on eukaryotic enzymes have been reviewed recently [8,40].

5. Sequence

In the CAZy database, the α-amylases are grouped with different kinds of glycosyl hydrolases in Family 13. In order to identify a sequence in this very large group as an α-amylase sequence, one ultimately needs experimental results. A more convenient approach, however, is to align the protein sequence in question to a known α-amylase sequence and look for conserved sequence patterns. α-Amylases sequences contain at least four such conserved patterns (numbered I–IV), which are found in the TIM-barrel on β-strands 3, 4 and 5 and in the loop connecting β-strand 7 to α-helix 7 (Fig. 3).

The residues that form region I (Fig. 4A) are found in the C-terminal end of the third β-strand of the TIM barrel (β3). This region contains the three fairly conserved amino acids Asp100, Asn104 and His105 (BLA numbering). Furthermore, there is a preference for Val at position 102, which is not readily explainable. Asp100 is important for the active site integrity, as it hydrogen-bonds to Arg229, which is a fully conserved residue within hydrogen-bond distance of both the catalytic nucleophile Asp231 and the proton donor Glu261. Asn104, on the other hand, does not participate directly in the stabilisation of the active site structure, but coordinates the conserved calcium ion between the A and B domains [22–24]. His105 stabilises the interaction between the C-terminal of β3 and the rest of the TIM-barrel by hydrogen bonding to Asn104 and to the backbone oxygen of Tyr56 (BLA numbering), which is situated in the loop connecting β2 to α2.

Region II (Fig. 4B) is located in β4 and contains the catalytic nucleophile Asp231 and the invariant residue Arg229. These two residues are found in all α-amylases and are believed to be indispensable for catalytic activity [40]. Lys234 and His235 are also found in this region. These two residues form part of subsite +2 and are thus supposed to bind the reducing end of the glucose chain in the substrate binding cleft [8,40].

Region III (Fig. 4C) includes the catalytic proton donor Glu261 and is positioned in the C-terminal part of the fifth β-strand of the TIM-barrel. Glu261 is the only totally conserved residue in this region.

The residues forming region IV (Fig. 4D) are situated in the loop connecting β7 to α7 and shield the active site from the solvent (Fig. 1). From visual inspection of α-amylase and CGTase X-ray structures with bound substrates, it seems likely that this loop has to move in order for the substrate to bind (see Fig. 1). The only fully conserved residue is Asp328, but there is a strong preference for His at position 327, while Phe, Val and Asn are very often seen at positions 323, 324 and 326, respectively. It has been suggested that Asp328 is involved in substrate binding, substrate distortion and in elevating the pK_a of Glu261 [41–43].

5.1. Other conserved regions

Janecek [44,45] has proposed that, in addition to the four conserved regions, there are two more conserved regions in the α-amylase sequences. One of these contains the aspartic acid involved in coordinating the conserved calcium ion, and the other region is a proposed hinge region in domain B. Since CGTases are structurally very similar to α-amylases, finding differences between the primary structures of CGTases and α-amylases has attracted considerable interest. Janecek et al. [46] have located three such features that can classify the amino acid sequence in most cases as either α-amylase or CGTase (Table 2).

6. Catalytic mechanism

α-Amylases cleave α1→4 glycosidic linkages with a net retention of the configuration around the

Table 2
Differences between α-amylase and CGTase sequences, according to Janecek et al. [46]

Asn104 (BLA numbering) is preceded by Ala–Pro or Thr–Pro in the CGTases. α-Amylases usually have Val instead of Ala/Thr
Asp100 (BLA numbering) is followed by Tyr or Phe in the CGTases
Arg229 (BLA numbering) is preceded by Ile
The residue three before Phe323 (BLA numbering) is Met or Gln in the CGTases, but is Ala, Leu or Ser in the α-amylases

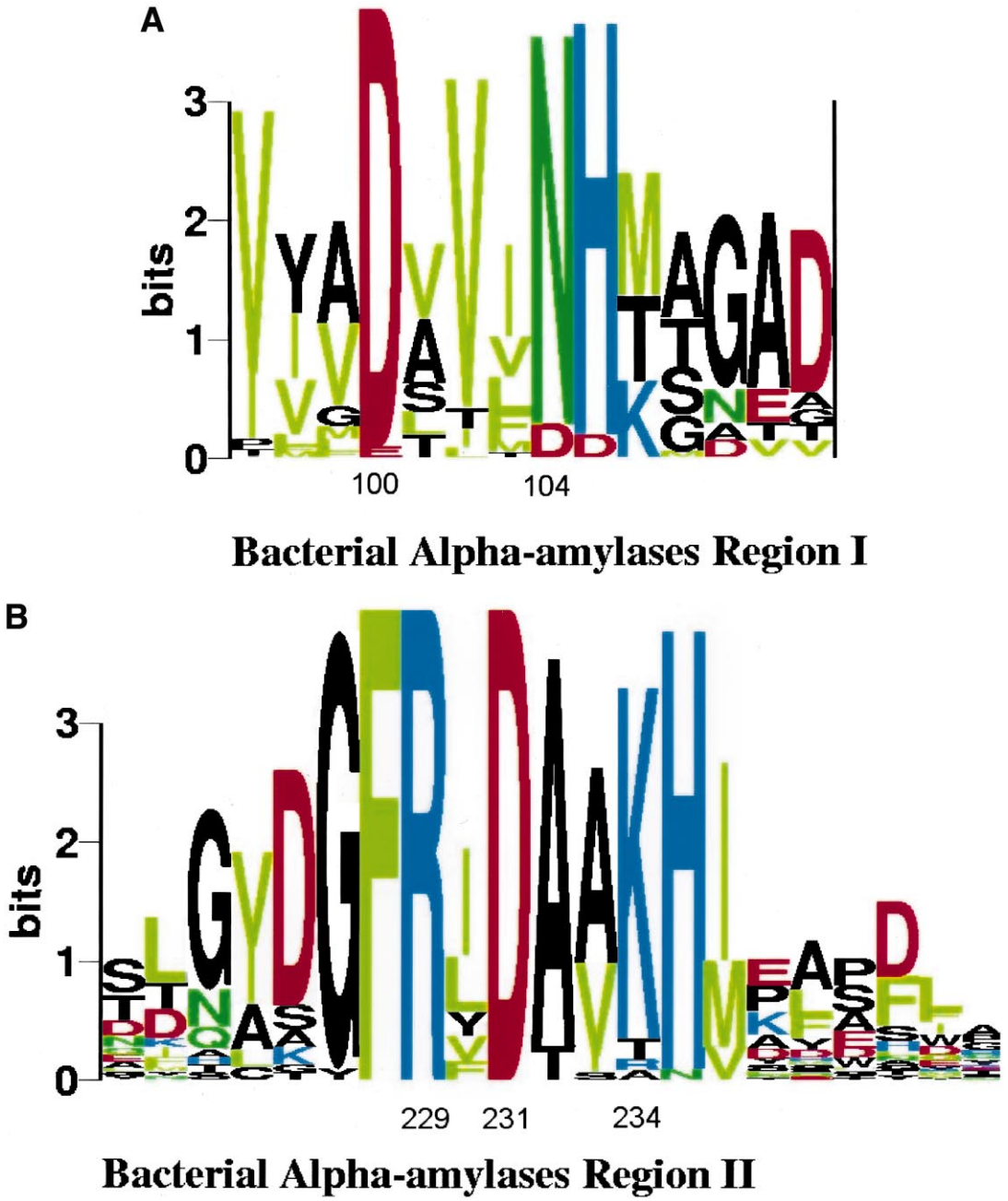

Fig. 4. Sequence logos of the four conserved sequence regions in bacterial α-amylases. Sequence numbers according to *Bacillus licheniformis* α-amylase. The sequence logos were created with the Delila software [91]. (A) Sequence logo plot of Region I. (B) Sequence logo plot of Region II. (C) Sequence logo plot of Region III. (D) Sequence logo plot of Region IV.

anomeric carbon atom of the sugar, i.e., the reducing end formed upon cleavage of the substrate is released in the α configuration. This behaviour is displayed by all retaining glycosyl hydrolases, for which the proposed catalytic mechanism [47–49] consists of three steps (Fig. 5). Step one is the protonation of the glycosidic oxygen by the proton donor (Glu261). This is followed by a nucleophilic attack on the C1 of the sugar residue in the −1 subsite by the catalytic nucleophile (Asp231) [50]. After the aglycon part of the substrate leaves, a water molecule is activated, presumably by the now deprotonated Glu261. This

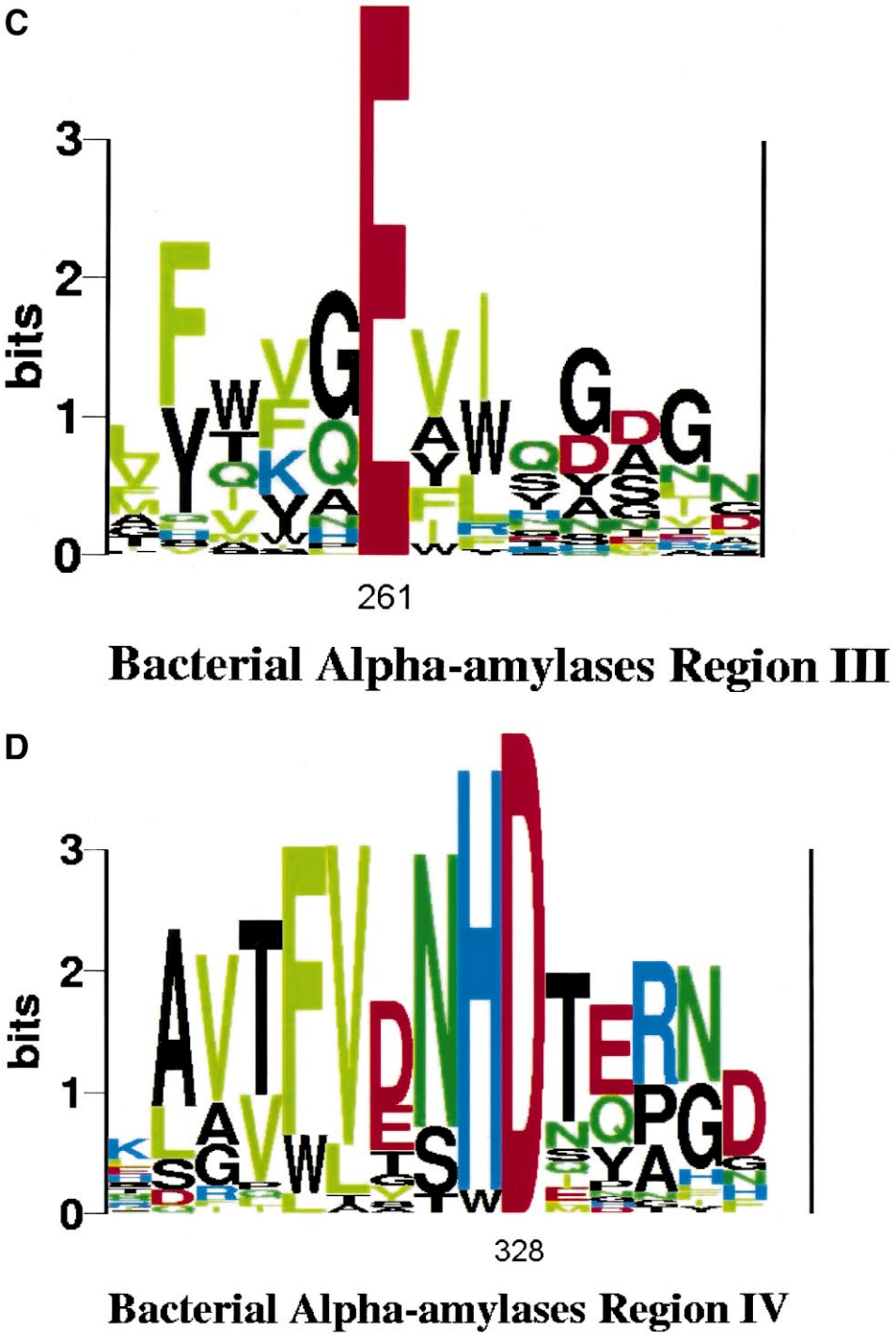

Fig. 4 (*continued*).

water molecule hydrolyses the covalent bond between the oxygen of the nucleophile and the C1 of the sugar residue, thus completing the catalytic cycle. The third conserved acid in the active site, Asp328, plays no direct role in this catalytic mechanism, but is nevertheless known to be important for catalysis [4]. It has been suggested that Asp328 elevates the pK_a of E261 [41–43] by means of electrostatic inter-

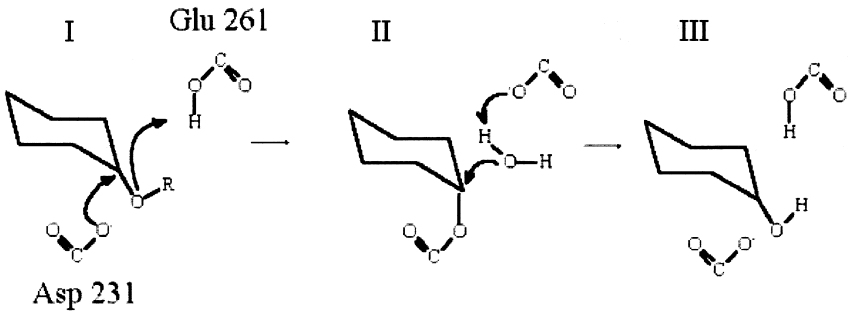

Fig. 5. Catalytic mechanism of retaining glycosyl hydrolases. (I) Protonation of the glycosidic oxygen and attack on the glucose C1 by D231. Departure of the reducing end of the substrate. (II) Activation of a water molecule, cleavage of C1-D231 covalent bond. (III) Regeneration of the initial protonation states.

actions. It has also been shown that Asp328 is involved in binding and distortion of the substrate [42,50].

Point mutations of the three catalytic acids have been used to establish their importance in the catalytic mechanism. Mutating one of these acids to the corresponding amide resulted in enzymes with an activity that was either heavily reduced [41,43] or completely absent [51,52]. It is still being debated whether these mutants are active or not [41,52,53], as this is of importance for the view of the catalytic mechanism [53]. It is possible that the activity measured for the acid→amide mutations originates from deamidation [54] of the mutated residue. It has been argued that the activity of active site mutants could originate from contamination by the wild type [52] or, in the case of alanine mutants, that a small buffer component (e.g., acetic acid) could substitute for the side chain that was removed.

We constructed four active site mutants in a chimaeric *Bacillus* α-amylase (D231A, E261A, D328A and D231A+E261A, BLA numbering) in order to resolve this question (Borchert, Nielsen, Frantzen, unpublished results). The mutants were purified to homogeneity as judged by SDS–PAGE. By using the standard insoluble blue starch assay (Phadebas α-amylase test, Pharmacia), we found α-amylase activity in all of the purified enzyme preparations (Table 3). Extreme care had been taken to eliminate all sources of wild-type contamination (new columns, filter, etc. were used), and none of the buffers contained nucleophilic components able to fill the hole produced by Asp→Ala or Glu→Ala mutants. An unexpectedly high activity for the double mutant and nearly identical pH-activity profiles for all mutants have led us to believe that the activity originates from a trace amount of an unidentified enzyme that co-purifies with the mutant α-amylases. This is further corroborated by the correlation between the purification yield and the specific activity (also see Knegtel et al. [43] who present similar results for a CGTase from *Bacillus circulans*, but come to the conclusion that the mutant enzymes are active). We cannot rule out, however, whether these mutant enzymes possess catalytic activity, but it is questionable whether the specific activities reported previously [41,43] originate solely from the mutant enzymes. Takase et al. [52] have clearly demonstrated that

Table 3
Activity of active site mutants in a chimaeric *Bacillus* α-amylase

Mutation(s)	Activity (mol^{-1})	Reduction in activity (factor)	Yield (mg)
None (wild type)	67000	–	–
D231A	7.3	9000	11.4
E261A	0.99	68000	156.7
D328A	4.0	17000	26.7
D231A+E261A	8.2	8000	14.3

Activity is reported in arbitrary units.

contamination by the wild type can be responsible for a large part of the catalytic activity displayed by a purified mutant enzyme preparation.

7. Stability engineering

Most of the industrial processes which involve the use of α-amylases, are carried out at rather extreme conditions with respect to temperature and pH, as illustrated in Section 1. Thus, the overall stability of these enzymes is an issue of significant interest and has been subjected to many studies, by industry and academia.

There are many reasons for the inactivation of α-amylases in industrial applications. Incubation at high temperatures is the primary cause of unfolding, but incubation at extreme pH values, exposure to metal-ion chelators and the exposure to oxidising agents can also result in denaturation [55–58]. Thermodynamic measurements of the stability of the α-amylases in the form of ΔG_{fold} values (the difference in free energy between the folded and unfolded state of the protein) has not been determined because the α-amylases unfold irreversibly in vitro. It has been proposed that the thermoinactivation of the *Bacillus* α-amylases is a two-stage process that involves an early reversible unfolding step which leads to a partially unfolded form of the enzyme. The reversible step is followed by an irreversible step that converts the partially unfolded form into an unfolded state, from which the folded conformation can no longer be reached [55,59,60]. The inability of the unfolded state to refold could be due to covalent modifications of the polypeptide chain or to very high energy barriers along the folding pathway.

A number of studies have addressed the stability and irreversible inactivation of the *Bacillus* α-amylases [55,59–61]. Primarily, the *B. lichenifomis* α-amylase (BLA), *B. amyloliquefaciens* α-amylase (BAA) and *B. stearothermophilus* α-amylase (BStA) have been subjected to such studies. Of these three, BLA is the most stable, followed by BStA and BAA respectively. Tomazic and Klibanov [60] looked at the effects of high temperature (90°C) at the optimum for enzymatic activity and proposed that the irreversible thermoinactivation of BAA and BStA is due to monomolecular scrambling rendering the molecule unable to refold. In the case of BLA, the primary cause of inactivation was found to be deamidation of asparagine and glutamine residues. Tomazic and Klibanov [60] propose that the enhanced stability of BLA is primarily due to additional salt-bridges involving the lysine residues K88, K253 and K385.

7.1. Metal ions

The effect of metal ions (especially calcium) and metal-ion chelators has also been examined. Lecker and Khan [57] looked at the residual activity of BStA after inactivation experiments with respect to temperature as well as protein and EDTA concentrations, and fitted experimental data to a two-stage model of the inactivation process. The first stage was the reversible disassociation of the calcium ion from the native protein, followed by irreversible denaturation at high temperatures.

7.2. Hybrid enzymes

A number of groups have generated hybrids between α-amylases as an elegant way of pinpointing regions of particular importance for the different properties of the individual enzymes [62–65]. BLA and BAA share more than 70% sequence identity and have primarily been used for these studies [62,63].

Suzuki et al. [62] identified two regions that were important for the higher thermo-stability of BLA in comparison to BAA. Based on amino acid differences observed in these two regions, three stabilising mutations in BAA were proposed: the deletion of R176 and G177, and the substitution K269A. Both of these mutations caused a significant and additive thermo-stabilisation of BAA. This R176-G177 deletion has been transferred to a number of other α-amylases derived from various *Bacillus* species. Similar effects on the thermo-stability were seen for these [56,66,67].

Conrad et al. [63] were able to pin-point four regions of particular importance for the thermo-stability of BLA, namely 34–76, 112–142, 174–179 and 263–276. Two of these coincide with the mutations identified earlier by Suzuki et al. [62], but none of these studies could support the predictions by Tomazic and Klibanov with respect to the important

lysine residues [60]. In fact, the removal of a lysine residue in BAA had a stabilising effect.

A number of the well-known stabilising mutation concepts have been successfully applied to α-amylases and are described below.

7.3. Stabilisation by the introduction of prolines

The introduction of prolines in loop regions is a general protein stabilising concept [68]. The stabilising effect is caused primarily by lowering the entropy of the unfolded state more than the entropy of the folded state. The insertion of proline residues is, of course, only possible if Pro can be accommodated in the structure. Arg124 (corresponding to Pro122 of BLA) in an α-amylase derived from an alkalophilic *Bacillus* species (NCIB 12512, 69% identical to BLA) is expected to be located in a β-turn with a geometry that could accommodate a proline residue. Not only did the R124P mutation stabilise the enzyme, but it was also shown to be additive with the two amino acid deletion [66]. Similar results have been obtained for the α-amylase from *Bacillus* species KSM-1378 [69].

7.4. Positions 133 and 209 in BLA

The most stable native *Bacillus* α-amylase, BLA, has been further stabilised with respect to withstand high temperature and acidic pH. Two positions, 133 and 209, have been identified as being important for the thermo-stability of BLA [70,71]. Twelve different amino acids were substituted for H133 by an elegant tRNA suppressor method, and H133Y was shown to improve the stability the most [71]. The A209V substitution was isolated after a random mutagenesis and screening approach. The stabilising effect of this mutation was shown to be additive with the H133Y mutation, so that the half-life of the double mutant was increased almost 10-fold at 90°C [70]. All naturally occurring amino acids were introduced in each of these two positions [72], and a number of the substitutions for H133 were shown to enhance the stability of BLA. Of these H133I had the largest effect, being even more stable than the H133Y mutant mentioned earlier. An equally fair agreement can be observed between the stabilising effect and both the hydrophobicity and the statistic pleated sheet propensity of the side chain introduced in position 133, although these explanations seem a bit speculative. At position 209 the stabilising effect was explained as the result of a hydrophobic crevice being filled on the surface of the protein [11].

7.5. Random mutagenesis

Consecutive rounds of random mutagenesis and screening have also been used to identify M15T and N188S as stabilising mutations of BLA [73]. A 23-fold stability enhancement was achieved (measured at pH 5.0 and 83°C in the presence of 5 mM $CaCl_2$) by combining these mutations with H133Y/A209V. Shaw et al. [73] also predict a stabilising effect for additional substitutions: A33S, A52S, N96Q, S148N and A379S. Very little data has been presented in support of this claim, however.

7.6. Calcium sites

Of the three metal ions found in the interface between the A and the B domains, the outermost Ca^{2+} is exposed to solvent. Alanine 181 is located on the surface of the molecule close to this calcium ion, and introducing a bulkier group at this position (A181T) was expected to stabilise BLA by burying the calcium deeper in the protein. The substitution did indeed stabilise BLA, and the effect was shown to be additive together with H156Y and A209V [56].

7.7. Deamidation

The removal of the amide containing side chains in BLA by mutations Q264S and N190F also enhanced the stability of the enzyme (N. Declerck, personal communication). This is in agreement with the predictions of Tomazic and Klibanov [60], although other explanations are possible. The effect of these substitutions was shown to be additive to the effect of some of the previously described mutations, such as A209V, H156Y and A181T [56].

7.8. Oxidation stability

Oxidation also has a demonstrated negative effect on the stability of α-amylases. Cysteine 362 was identified as the oxidation prone residue in BStA [55,61],

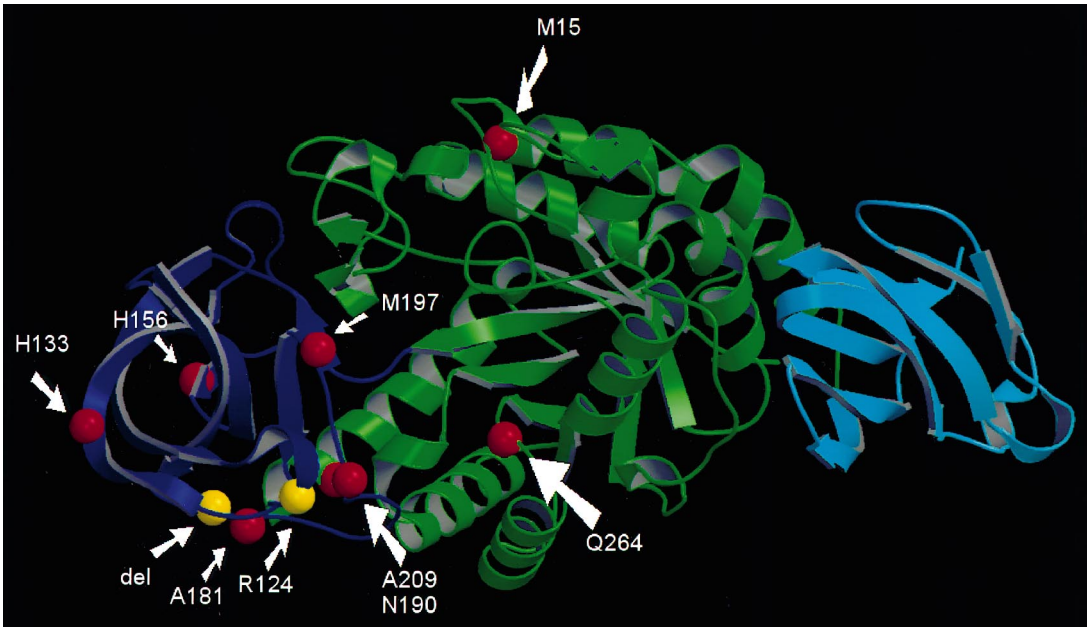

Fig. 6. Location of the stabilising mutations in BLA. Domain B is shown in blue, and domain C is shown in cyan. The locations of the stabilising mutations in BLA (M15, H133, H156, A181, N188, N190, A209, M197, Q264) are shown in red. The position of R124 and the location of the two-amino-acid deletion (del) is shown in yellow. The figure was prepared with the Molscript [89] and Raster3D [90] programs.

and methionine 197, which is situated close to the active site, has been shown to be responsible for the inactivation of BLA [58]. The introduction of any non-sulphur-containing amino acid at position 197 was shown to greatly reduce the oxidation sensitivity of BLA. The specific activity was, however, very much dependent on the introduced side chain, with an apparent preference for the smaller side chains [58].

7.9. *Clustering of stabilising mutations*

Random mutagenesis, homology considerations and rational protein engineering have been utilised to stabilise a number of different α-amylases. The additive nature of the stabilising mutations suggests that they affect the same reversible unfolding step. It is likely that this step is the first stage of the two-step inactivation model proposed by Tomazic and Klibanov [55]

Domain B, constituting residues 104–205 (BLA numbering), seems to be of major importance to the overall stability of α-amylases derived from the genus *Bacillus*. The majority of the stabilising mutations identified so far (see above description) seem to cluster within this domain of the molecule (see Fig. 6). One can speculate that the initial reversible step is a partial unfolding of the B-domain, which seems to be the 'weak' part of the molecule.

8. Engineering pH-activity profiles

Many industrial processes are carried out at extreme pH values, and the successful use of α-amylases in such processes is, of course, dependent on having an enzyme that is both stable and active at the pH value in question. As shown in the previous section, stability at extreme pH values can be engineered by normal protein stability engineering techniques such as helix capping, removal of deamidating residues [11,56,70,72] and cavity-filling. It is important, however, to realise that special phenomena are likely to destabilise the protein at extreme pH values, and that preventing these phenomena can have a great effect on the stability of the enzyme. The most important of these phenomena are the spontaneous formation of peptide succinimides in both

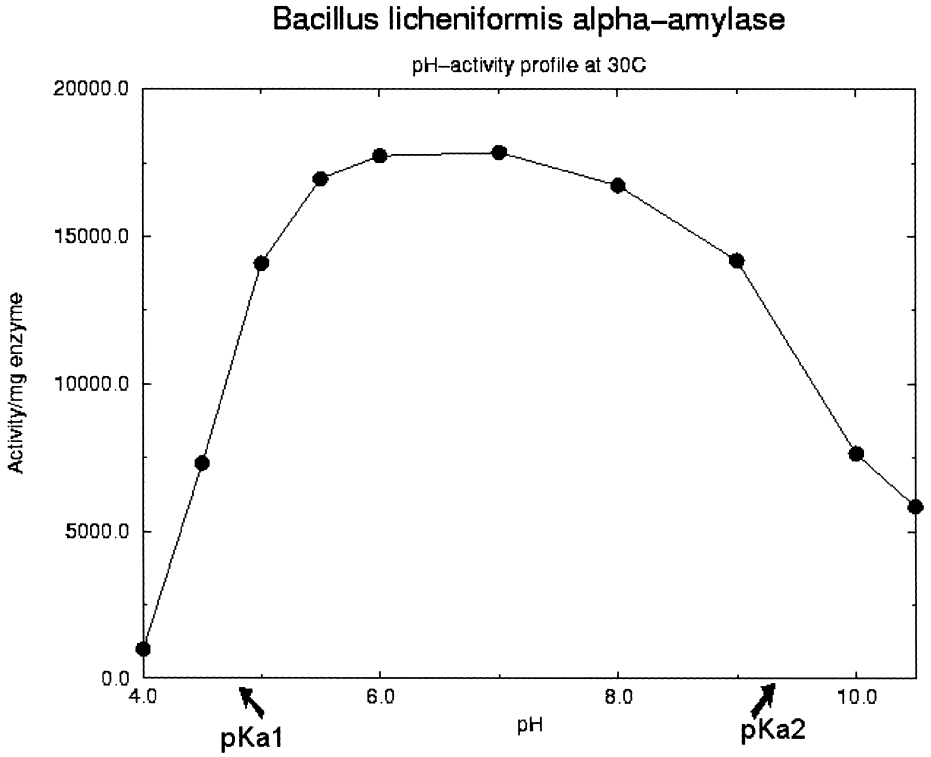

Fig. 7. The pH-activity profile of *Bacillus licheniformis* α-amylase with the indication of the approximate values of pK_{a1} and pK_{a2}. The activity is shown in arbitrary values.

Asp–Gly and Asn–Gly sequences [74], the burial of ionised groups [75,76] and the repulsive electrostatic forces associated with the large net charges of the protein found at both acidic and basic pH [77]. It is currently believed that the repulsive electrostatic energies between charged groups at extreme pH values contribute less to the decrease in stability than the energy associated with the burial of ionised groups [75].

Stability is a prerequisite for activity at extreme pH values, but it alone is not sufficient, as the active site residues must be in a catalytically competent protonation state in order for the enzyme to be active. Thus, the proton donor (Glu261) is required to be protonated, while the nucleophile (Asp231) must be negatively charged. The bell-shaped pH-activity profiles displayed by the α-amylases [42,78,79] have led to the assumption that the acidic limb of the pH-activity profile is determined by the titration of the catalytic nucleophile, and that the basic limb reflects the titration of the catalytic proton donor (Fig. 7). Recent experimental evidence supporting this hypothesis comes from studies on *Bacillus circulans* xylanase, where the pK_a value of the proton donor has been shown to be coincident with the apparent pK_a value of the drop in catalysis at high pH [80].

Therefore, if an α-amylase is stable over the entire pH range, it is conceivable that the pH-activity profile can be changed if the pK_a value of either the nucleophile or the proton donor is changed. pK_a values can be changed by altering the electrostatic field experienced by a titratable group [81], and both the local hydrogen bonding network and the solvent accessibility of the titratable group as well as other charged groups influence the electrostatic field. Typically, charged residues are inserted in the vicinity of the titratable group [82–85], although changing the immediate environment in a subtler way has been attempted [83,86]. Mutagenesis experiments that insert or remove charged residues near to or in the active site have been carried out on CGTases [16,43] and α-amylases [83,87], but no predictable way of changing the pH-activity profile has been found.

Wind et al. [16] report identical downward shifts in the pK_a value of the proton donor for a mutant

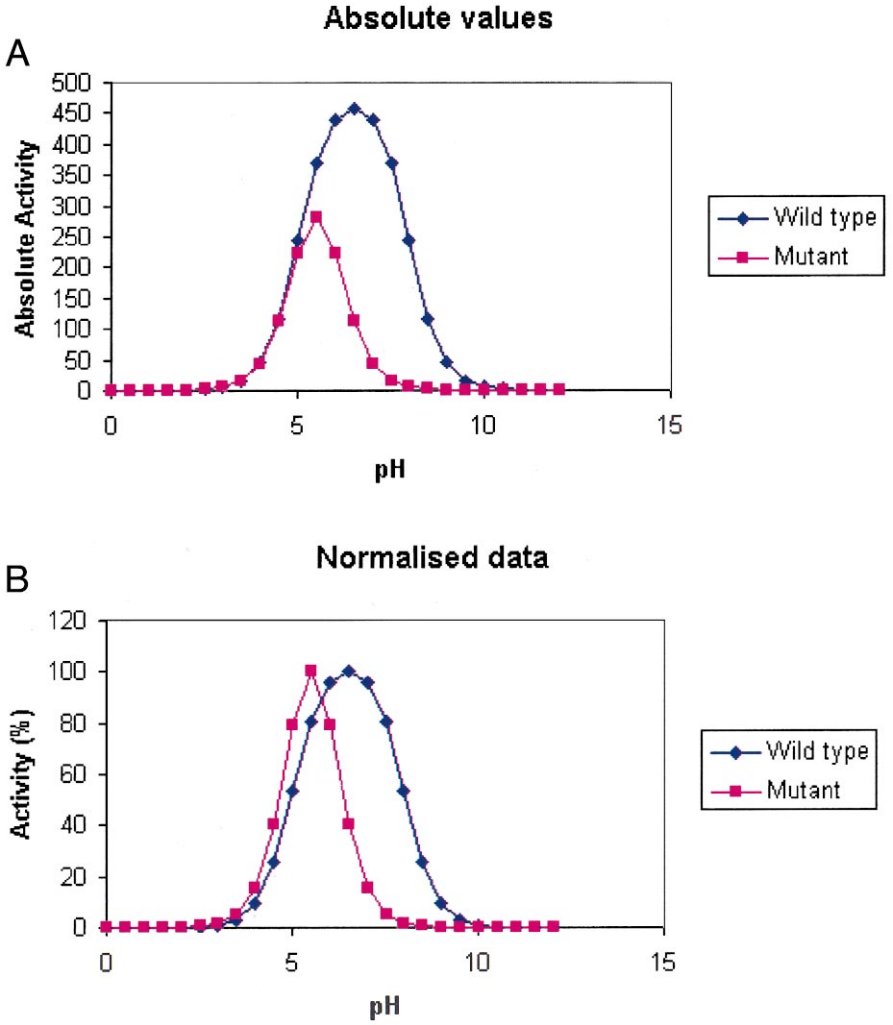

Fig. 8. pH-activity profiles for a hypothetical wild-type enzyme and a mutant that changes the pK_a value of the basic limb by two units. pK_a values for the wild type are pK_{a1} = 5.0 and pK_{a2} = 8.0. Mutant pK_a values are pK_{a1} = 5.0 and pK_{a2} = 6.0. The enzymatic activity was calculated using the formula

$$\text{Activity} = \text{Activity}_{\text{MAX}}\left(1-\frac{1}{1+10^{\text{p}K_{a1}-\text{pH}}}\right)\times\left(\frac{1}{1+10^{\text{p}K_{a2}-\text{pH}}}\right)$$

where $\text{Activity}_{\text{MAX}}$ was set to an arbitrary value which was the same for both the wild-type and the mutant enzyme. The absolute plot (A) clearly gives the correct picture and should be used wherever possible. Many mutant enzyme activities are orders of magnitude smaller than the wild-type activity, and in such cases the absolute pH-activity profiles are not easily plotted on the same graph. Neither the logarithmic plot (C) nor the wild-type normalised plot (D) are hampered by this, and can thus be used to analyse the data correctly, whereas the normalised plot (B) will produce misleading graphs under many circumstances.

inserting a positive charge in the active site (F283K), and for a mutant inserting a negative charge in the active site (N329D). It is remarkable that both mutants produce a downward shift, as theory predicts that the insertion of a negative charge produces an upward shift in the pK_a value of the proton donor. Wind et al. [16] speculate that the seemingly contradictory results for N329D are due to the binding of an H_3O^+ ion in the active site which supposedly interacts with the proton donor and thus lowers the pK_a of this residue.

In another study [83], 14 site-directed mutations were constructed in BLA in order to change the pH-activity profile. The mutants were designed so

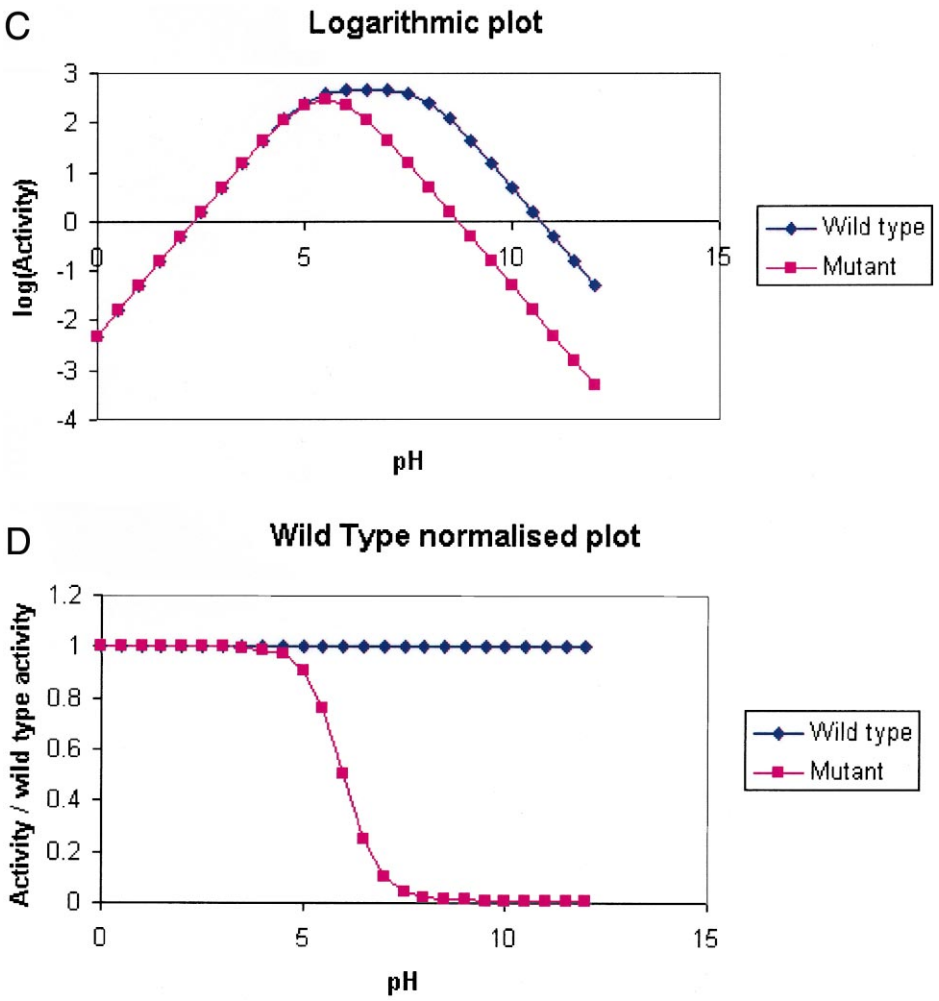

Fig. 8 (*continued*).

as to either perturb the electrostatic field in the active site by means of long range electrostatic forces (insertion of charged amino acids at a distance from the catalytic acids), or to change either the solvent accessibility of the catalytic nucleophile or the local hydrogen bonding network environment of this residue. The pH-activity profile shifts found for these mutants were smaller than the shifts reported by Wind et al. [16], but most mutants were just as active as the wild type. In several cases, the direction of the pH-activity profile shifts predicted by electrostatic calculations [88] and the direction of the observed shifts were the exact opposite and is thus similar to the Wind et al. data. On the basis of the BLA mutants, it was concluded that factors other than electrostatic effects play a significant role in determining the pH-activity profile of BLA.

A study by Takase [37] has shown that mutation of Asn329 to Lys or Asp in BStA (BLA Asn326) can change the pH-activity profile quite significantly. It is, however, also difficult to explain the pH-activity profile shifts for these mutants.

It is important, however, that care is taken when comparing pH-activity profiles (Fig. 8) since wrong conclusions can be drawn when some plotting methods are used.

9. Conclusion

The use of bacterial α-amylases has become more widespread in recent years due to the highly optimised α-amylases constructed by means of protein engineering techniques. In particular, a number of

mutations within domain B have improved the stability of BLA to the extent that it can be used for almost any high-temperature application. It is difficult to rationalise the stabilising effect for several of the stabilising mutations, and the processes leading to the irreversible denaturation of the α-amylases are still unknown. In this respect, there are still many questions to be answered regarding the stability of bacterial α-amylases.

With the construction of the highly stable *Bacillus* α-amylases, it is likely, however, that the future will see a change in the focus of α-amylase engineering. Enzymes with specific pH-activity profiles and tailor-made substrate and product specificities will undoubtedly be welcome in many industrial applications, and we therefore predict that the focus of α-amylase engineering will shift from stability engineering to these new areas. Initial studies have been made in both pH-activity profile engineering and substrate specificity engineering, as mentioned in the previous sections. But whereas many well-proven strategies for stabilising a protein have already been developed, it seems that there is a shortage of theories and methods for addressing the engineering of both substrate specificities and pH-activity profiles. Given the continuing research efforts in the α-amylase field it seems likely, however, that such theories and methods will be rapidly developed and result in the construction of α-amylases with novel, improved properties.

Acknowledgements

The authors wish to thank Nathalie Declerck for sharing her unpublished results with us, and Gert Vriend for his critical reading of the manuscript.

References

[1] M.A. Huynen, T. Dandekar, P. Bork, Variation and evolution of the citric-acid cycle: a genomic perspective, Trends Microbiol. 7 (1999) 281–291.
[2] T. Dandekar, S. Schuster, B. Snel, M. Huynen, P. Bork, Pathway alignment: application to the comparative analysis of glycolytic enzymes, Biochem. J. 343 (1999) 115–124.
[3] M. Vihinen, P. Mantsala, Microbial amylolytic enzymes, Crit. Rev. Biochem. Mol. Biol. 24 (1989) 329–418.
[4] P.M. Coutinho, B. Henrissat, Carbohydrate-active enzymes: an integrated database approach, in: H.J. Gilbert, G. Davies, B. Henrissat, B. Svensson (Eds.), Recent Advances in Carbohydrate Bioengineering, The Royal Society of Chemistry, Cambridge, 1999, pp. 3–12.
[5] N. Ramasubbu, V. Paloth, Y. Luo, G.D. Brayer, M.J. Levine, Structure of human salivary α-amylase at 1.6 Å resolution: implications for its role in the oral cavity, Acta Cryst. D52 (1996) 435–446.
[6] G.D. Brayer, Y. Luo, S.G. Withers, The structure of human pancreatic α-amylase at 1.8 A resolution and comparisons with related enzymes, Protein Sci. 4 (1995) 1730–1742.
[7] H. Guzman-Maldonado, O. Paredes-Lopez, Amylolytic enzymes and products derived from starch: a review, Crit. Rev. Food Sci. Nutr. 35 (1995) 373–403.
[8] B. Svensson, M. Søgaard, Protein engineering of amylases, Biochem. Soc. Trans. 20 (1992) 34–42.
[9] N. Aghajari, G. Feller, C. Gerday, R. Haser, Crystal structures of the psychrophilic α-amylase from *Alteromonas haloplanctis* in its native form and complexed with an inhibitor, Protein Sci. 7 (1998) 564–572.
[10] G. Feller, T. Lonhienne, C. Deroanne, C. Libioulle, J. Van Beeumen, C. Gerday, Purification, characterization, and nucleotide sequence of the thermolabile α-amylase from the antarctic psychrotroph *Alteromonas haloplanctis* A23, J. Biol. Chem. 267 (1992) 5217–5221.
[11] N. Declerck, M. Machius, R. Chambert, G. Wiegand, R. Huber, C. Gaillardin, Hyperthermostable mutants of *Bacillus licheniformis* α-amylase: thermodynamic studies and structural interpretation, Protein Eng. 10 (1997) 541–549.
[12] F. Uchino, A thermophilic and unusually acidophilic amylase produced by a thermophilic acidophilic *Bacillus sp.*, Agric. Biol. Chem. 46 (1982) 7–13.
[13] K. Horikoshi, Production of alkaline enzymes by alkalophilic microorganisms. Part II. Alkaline amylase produced by *Bacillus* No. A-40-2, Agric. Biol. Chem. 35 (1971) 1783–1791.
[14] M.B. Ingle, R.J. Erickson, Bacterial α-amylases, Adv. Appl. Microbiol. 24 (1978) 257–278.
[15] H.J. Cha, H.G. Yoon, Y.W. Kim, H.S. Lee, J.W. Kim, K.S. Kweon, B.H. Oh, K.H. Park, Molecular and enzymatic characterization of a maltogenic amylase that hydrolyzes and transglycosylates acarbose, Eur. J. Biochem. 253 (1998) 251–262.
[16] R.D. Wind, J.C. Uitdehaag, R.M. Buitelaar, B.W. Dijkstra, L. Dijkhuizen, Engineering of cyclodextrin product specificity and pH optima of the thermostable cyclodextrin glycosyltransferase from *Thermoanaerobacterium thermosulfurigenes* EM1, J. Biol. Chem. 273 (1998) 5771–5779.
[17] D. Penninga, B. Strokopytov, H.J. Rozeboom, C.L. Lawson, B.W. Dijkstra, J. Bergsma, L. Dijkhuizen, Site-directed mutations in tyrosine 195 of cyclodextrin glycosyltransferase from *Bacillus circulans* strain 251 affect activity and product specificity, Biochemistry 34 (1995) 3368–3376.
[18] H. Nakatani, Monte Carlo simulation of multiple attack mechanism of α-amylase, Biopolymers 39 (1996) 665–669.

[19] B. Henrissat, A classification of glycosyl hydrolases based on amino acid sequence similarities, Biochem. J. 280 (1991) 309–316.
[20] S. Janecek, B. Svensson, B. Henrissat, Domain evolution in the α-amylase family, J. Mol. Evol. 45 (1997) 322–331.
[21] E.A. MacGregor, α-amylase structure and activity, J. Protein Chem. 7 (1988) 399–415.
[22] E. Boel, L. Brady, A.M. Brzozowski, Z. Derewenda, G.G. Dodson, V.J. Jensen, S.B. Petersen, H. Swift, L. Thim, H.F. Woldike, Calcium binding in α-amylases: an X-ray diffraction study at 2.1-Å resolution of two enzymes from *Aspergillus*, Biochemistry 29 (1990) 6244–6249.
[23] M. Machius, G. Wiegand, R. Huber, Crystal structure of calcium-depleted *Bacillus licheniformis* α-amylase at 2.2 Å resolution, J. Mol. Biol. 246 (1995) 545–559.
[24] M. Machius, N. Declerck, R. Huber, G. Wiegand, Activation of *Bacillus licheniformis* α-amylase through a disorder-→order transition of the substrate-binding site mediated by a calcium-sodium-calcium metal triad, Structure 6 (1998) 281–292.
[25] B.L. Vallee, E.A. Stein, W.N. Summerwill, E.H. Fischer, Metal content of α-amylases of various origins, J. Biol. Chem. 234 (1959) 2901–2905.
[26] G. Feller, F. Payan, F. Theys, M. Qian, R. Haser, C. Gerday, Stability and structural analysis of α-amylase from the antarctic psychrophile *Alteromonas haloplanctis* A23, Eur. J. Biochem. 222 (1994) 441–447.
[27] A. Levitsky, M.L. Steer, The allosteric activation of mammalian α-amylase by chloride, Eur. J. Biochem. 41 (1974) 171–180.
[28] S.B. Larson, A. Greenwood, D. Cascio, J. Day, A. McPherson, Refined molecular structure of pig pancreatic α-amylase at 2.1 Å resolution, J. Mol. Biol. 235 (1994) 1560–1584.
[29] G. Buisson, E. Duee, R. Haser, F. Payan, Three dimensional structure of porcine pancreatic α-amylase at 2.9 Å resolution. Role of calcium in structure and activity, EMBO J. 6 (1987) 3909–3916.
[30] A. Kadziola, M. Søgaard, B. Svensson, R. Haser, Molecular structure of a barley α-amylase-inhibitor complex: implications for starch binding and catalysis, J. Mol. Biol. 278 (1998) 205–217.
[31] A.M. Brzozowski, D.M. Lawson, J.P. Turkenburg, H. Bisgaard-Frantzen, A. Svendsen, T.V. Borchert, Z. Dauter, K.S. Wilson, G.J. Davies, Structural analysis of a chimeric bacterial α-amylase. High resolution analysis of native and ligand complexes, Biochemistry 39 (2000) 9099–9107.
[32] G. Feller, O. Bussy, C. Houssier, C. Gerday, Structural and functional aspects of chloride binding to *Alteromonas haloplanctis* α-amylase, J. Biol. Chem. 271 (1996) 23836–23841.
[33] G.J. Davies, K.S. Wilson, B. Henrissat, Nomenclature for sugar-binding subsites in glycosyl hydrolases, Biochem. J. 321 (1997) 557–559.
[34] Z. Dauter, M. Dauter, A.M. Brzozowski, S. Christensen, T.V. Borchert, L. Beier, K.S. Wilson, G.J. Davies, X-ray structure of Novamyl, the five-domain 'maltogenic' α-amylase from *Bacillus stearothermophilus*: maltose and acarbose complexes at 1.7 Å resolution, Biochemistry 38 (1999) 8385–8392.
[35] A.M. Brzozowski, G.J. Davies, Structure of the *Aspergillus oryzae* α-amylase complexed with the inhibitor acarbose at 2.0 Å resolution, Biochemistry 36 (1997) 10837–10845.
[36] M. Vihinen, P. Ollikka, J. Niskanen, P. Meyer, I. Suominen, M. Karp, L. Holm, J. Knowles, P. Mantsala, Site-directed mutagenesis of a thermostable α-amylase from *Bacillus stearothermophilus*: putative role of three conserved residues, J. Biochem. (Tokyo) 107 (1990) 267–272.
[37] K. Takase, Effect of mutation of an amino acid residue near the catalytic site on the activity of *Bacillus stearothermophilus* α-amylase, Eur. J. Biochem. 211 (1993) 899–902.
[38] R.D. Dua, S. Kochhar, Substrate binding nodes of *Bacillus amyloliquefaciens* α-amylase, Indian J. Biochem. Biophys. 23 (1986) 133–139.
[39] T. Suganuma, M. Ohnishi, K. Hiromi, T. Nagahama, Elucidation of the subsite structure of bacterial saccharifying α-amylase and its mode of degradation of maltose, Carbohydr. Res. 282 (1996) 171–180.
[40] B. Svensson, Protein engineering in the α-amylase family: catalytic mechanism, substrate specificity, and stability, Plant Mol. Biol. 25 (1994) 141–157.
[41] C. Klein, J. Hollender, H. Bender, G.E. Schulz, Catalytic center of cyclodextrin glycosyltransferase derived from X-ray structure analysis combined with site-directed mutagenesis, Biochemistry 31 (1992) 8740–8746.
[42] B. Strokopytov, D. Penninga, H.J. Rozeboom, K.H. Kalk, L. Dijkhuizen, B.W. Dijkstra, X-ray structure of cyclodextrin glycosyltransferase complexed with acarbose. Implications for the catalytic mechanism of glycosidases, Biochemistry 34 (1995) 2234–2240.
[43] R. M Knegtel, B. Strokopytov, D. Penninga, O.G. Faber, H.J. Rozeboom, K.H. Kalk, L. Dijkhuizen, B.W. Dijkstra, Crystallographic studies of the interaction of cyclodextrin glycosyltransferase from *Bacillus circulans* strain 251 with natural substrates and products, J. Biol. Chem. 270 (1995) 29256–29264.
[44] S. Janecek, New conserved amino acid region of α-amylases in the third loop of their (β/α)8-barrel domains, Biochem. J. 288 (1992) 1069–1070.
[45] S. Janecek, Invariant glycines and prolines flanking in loops the strand β2 of various (α/β)8-barrel enzymes: a hidden homology?, Protein Sci. 5 (1996) 1136–1143.
[46] S. Janecek, E.A. MacGregor, B. Svensson, Characteristic differences in the primary structure allow discrimination of cyclodextrin glucanotransferases from α-amylases, Biochem. J. 305 (1995) 685–686.
[47] M.L. Sinnott, Catalytic mechanisms of enzymic glycosyl transfer, Chem. Rev. 90 (1990) 1171–1202.
[48] J.D. McCarter, S.G. Withers, Mechanisms of enzymatic glycoside hydrolysis, Curr. Opin. Struct. Biol. 4 (1994) 885–892.
[49] G. Davies, B. Henrissat, Structures and mechanisms of glycosyl hydrolases, Structure 3 (1995) 853–859.
[50] J.C. Uitdehaag, R. Mosi, K.H. Kalk, B.A. van der Veen, L.

Dijkhuizen, S.G. Withers, B.W. Dijkstra, X-ray structures along the reaction pathway of cyclodextrin glycosyltransferase elucidate catalysis in the α-amylase family, Nat. Struct. Biol. 6 (1999) 432–436.
[51] A. Nakamura, K. Haga, S. Ogawa, K. Kuwano, K. Kimura, K. Yamane, Functional relationships between cyclodextrin glucanotransferase from an alkalophilic *Bacillus* and α-amylases. Site-directed mutagenesis of the conserved two Asp and one Glu residues, FEBS Lett. 296 (1992) 37–40.
[52] K. Takase, T. Matsumoto, H. Mizuno, K. Yamane, Site-directed mutagenesis of active site residues in *Bacillus subtilis* α-*amylase, Biochim. Biophys. Acta 1120 (1992) 281–288.*
[53] T. Kuriki, T. Imanaka, The concept of the α-amylase family: structural similarity and common catalytic mechanism, J. Biosci. Bioeng. 87 (1999) 557–565.
[54] T.E. Creighton, Proteins: Structures and Molecular Properties, 2nd ed., W.H. Freeman, New York, 1993, ch. 9.
[55] S.J. Tomazic, A.M. Klibanov, Mechanisms of irreversible thermal inactivation of *Bacillus* α-amylases, J. Biol. Chem. 263 (1988) 3086–3091.
[56] H. Bisgaard-Frantzen, A. Svendsen, B. Norman, S. Pedersen, S. Kjærulff, H. Outtrup, T.V. Borchert, Development of industrially important α-amylases, J. Appl. Glycosci. 46 (1999) 199–206.
[57] D.N. Lecker, A. Khan, Model for inactivation of α-amylase in the presence of salts: theoretical and experimental studies, Biotechnol. Prog. 14 (1998) 621–625.
[58] T.V. Borchert, S.F. Lassen, A. Svendsen, H. B. Frantzen, Oxidation stable amylases for detergents, in: S.B. Petersen, B. Svensson, S. Pedersen (Eds.), Carbohydrate Bioengineering, Elsevier Science, Amsterdam, 1995, pp. 175–179.
[59] M. Violet, J.C. Meunier, Kinetic study of the irreversible thermal denaturation of *Bacillus licheniformis* α-amylase, Biochem. J. 263 (1989) 665–670.
[60] S.J. Tomazic, A.M. Klibanov, Why is one *Bacillus* α-amylase more resistant against irreversible thermoinactivation than another?, J. Biol. Chem. 263 (1988) 3092–3096.
[61] M.P. Brosnan, C.T. Kelly, W.M. Fogarty, Investigation of the mechanisms of irreversible thermoinactivation of *Bacillus stearothermophilus* α-amylase, Eur. J. Biochem. 203 (1992) 225–231.
[62] Y. Suzuki, N. Ito, T. Yuuki, H. Yamagata, S. Udaka, Amino acid residues stabilizing a *Bacillus* α-amylase against irreversible thermoinactivation, J. Biol. Chem. 264 (1989) 18933–18938.
[63] B. Conrad, V. Hoang, A. Polley, J. Hofemeister, Hybrid *Bacillus amyloliquefaciens*×*Bacillus licheniformis* α-amylases. Construction, properties and sequence determinants, Eur. J. Biochem. 230 (1995) 481–490.
[64] B. Diderichsen, H. Outtrup, M. Schulein, B.E. Norman, Chimeric enzymes, European patent EP87305781 (1987).
[65] M.W. Rey, C. Requadt, S.E. Mainzer, M.H. Lamsa, E. Ferrari, P.J. Lad, L.G. Gray, Homologous α-amylases of *Bacillus* and generation of their hybrids in vivo, in: A.T. Ganesan, J.T. Hoch (Eds.), *Bacillus* Molecular Genetic and Biotechnology Applications, pp. 229–239.
[66] H. Bisgård-Frantzen, A. Svendsen, T.V. Borchert, Amylase variants, Patent WO96/23873 (1996).
[67] K. Igarashi, Y. Hatada, K. Ikawa, H. Araki, T. Ozawa, T. Kobayashi, K. Ozaki, S. Ito, Improved thermo-stability of a *Bacillus* α-amylase by deletion of an arginine-glycine residue is caused by enhanced calcium binding, Biochem. Biophys. Res. Commun. 248 (1998) 372–377.
[68] B.W. Matthews, H. Nicholson, W.J. Becktel, Enhanced protein thermo-stability from site-directed mutations that decrease the entropy of unfolding, Proc. Natl. Acad. Sci. USA 84 (1987) 6663–6667.
[69] K. Igarashi, Thermostabilization by proline substitution in an alkaline, liquefying α-amylase from *Bacillus sp*. strain KSM-1378, Biosci. Biotechnol. Biochem. 63 (1999) 1535–1540.
[70] P. Joyet, N. Declerck, C. Gaillardin, Hyperthermostable variants of a highly thermostable α-amylase, Biotechnology 10 (1992) 1579–1583.
[71] N. Declerck, P. Joyet, C. Gaillardin, J.M. Masson, Use of amber suppressors to investigate the thermo-stability of *Bacillus licheniformis* α-amylase. Amino acid replacements at 6 histidine residues reveal a critical position at His-133, J. Biol. Chem. 265 (1990) 15481–15488.
[72] N. Declerck, P. Joyet, J.Y. Trosset, J. Garnier, C. Gaillardin, Hyperthermostable mutants of *Bacillus licheniformis* α-amylase: multiple amino acid replacements and molecular modelling, Protein Eng. 8 (1995) 1029–1037.
[73] A. Shaw, R. Bott, A.G. Day, Protein engineering of α-amylase for low pH performance, Curr. Opin. Biotechnol. 10 (1999) 349–352.
[74] T.E. Creighton, Proteins: Structures and Molecular Properties, 2nd ed., W.H. Freeman, New York, 1993, ch. 10.
[75] A.S. Yang, B. Honig, On the pH dependence of protein stability, J. Mol. Biol. 231 (1993) 459–474.
[76] C. Tanford, Protein denaturation part C. Theoretical models for the mechanism of denaturation, Adv. Protein Chem. 25 (1970) 1–95.
[77] K. Linderstrøm-Lang, The ionization of proteins, C. R. Trav. Lab. Carlsberg Ser. Chim. 15 (1924) 1–29.
[78] T. Takagi, H. Toda, T. Isemura, in: P.D. Boyer (Ed.), Bacterial and Mold Amylases in The Enzymes, 3rd ed., 1971, pp. 235–271.
[79] M. Qian, R. Haser, G. Buisson, E. Duee, F. Payan, The active center of a mammalian α-amylase. Structure of the complex of a pancreatic α-amylase with a carbohydrate inhibitor refined to 2.2-Å resolution, Biochemistry 33 (1994) 6284–6294.
[80] L.P. McIntosh, G. Hand, P.E. Johnson, M.D. Joshi, M. Korner, L.A. Plesniak, L. Ziser, W.W. Wakarchuk, S.G. Withers, The pK_a of the general acid/base carboxyl group of a glycosidase cycles during catalysis: a ^{13}C-NMR study of *Bacillus circulans* xylanase, Biochemistry 35 (1996) 9958–9966.
[81] K. Linderstrøm-Lang, S.O. Nielsen, in: M. Bier (Ed.), Acid–Base Equilibria of Proteins in Electrophoresis, Academic, New York, 1959, pp. 35–89.

[82] S.E. Jackson, A.R. Fersht, Contribution of long-range electrostatic interactions to the stabilization of the catalytic transition state of the serine protease subtilisin BPN′, Biochemistry 32 (1993) 13909–13916.
[83] J.E. Nielsen, L. Beier, D. Otzen, T.V. Borchert, H.B. Frantzen, K.V. Andersen, A. Svendsen, Electrostatics in the active site of an α-amylase, Eur. J. Biochem. 264 (1999) 816–824.
[84] T.Y. Fang, C. Ford, Protein engineering of *Aspergillus awamori* glucoamylase to increase its pH optimum, Protein Eng. 11 (1998) 383–388.
[85] U. Bakir, P.M. Coutinho, P.A. Sullivan, C. Ford, P.J. Reilly, Cassette mutagenesis of *Aspergillus awamori* glucoamylase near its general acid residue to probe its catalytic and pH properties, Protein Eng. 6 (1993) 939–946.
[86] D.W. Urry, D.C. Gowda, S. Peng, T.M. Parker, N. Jing, R.D. Harris, Nanometric design of extraordinary hydrophobic-induced pK_a shifts for aspartic acid: relevance to protein mechanisms, Biopolymers 34 (1994) 889–896.
[87] M. Sogaard, A. Kadziola, R. Haser, B. Svensson, Site-directed mutagenesis of histidine 93, aspartic acid 180, glutamic acid 205, histidine 290, and aspartic acid 291 at the active site and tryptophan 279 at the raw starch binding site in barley α-amylase 1, J. Biol. Chem. 268 (1993) 22480–22484.
[88] B. Honig, K. Sharp, A.S. Yang, Macroscopic models of aqueous solutions: biological and chemical applications, J. Phys. Chem. 97 (1993) 1101–1109.
[89] http://www.avatar.se/molscript/
[90] http://www.bmsc.washington.edu/raster3d/
[91] http://www.lecb.ncifcrf.gov/–toms/delila.html